2-2 Electron Cyclotron Emission measurements by means of a Grating Polychromator on the Large Helical Device

P.C. de Vries, K. Kawahata, Y. Nagayama, S. Inagaki, H. Sasao and Y Ito

National Institute for Fusion Science, 322-6 Oroshi-cho, Toki-shi, 509-5292 Japan

The electron cyclotron emission (ECE) spectrum at the Large Helical Device (LHD) is measured by a 14-channel grating polychromator. During standard operation the polychromator monitors 2nd harmonic frequencies (100 - 150 GHz) with a spectral resolution of 1.5 GHz. At sufficient high density the 2nd harmonic X-mode polarisation is optically thick and can be used to determine the temperature profile. However, the large magnetic field shear in LHD affects the ECE polarisation. This effect has been studied numerically. The wave polarisation was found to rotate in the laboratory frame. Experiments have been carried out by means of a polarisation rotator in the diagnostic waveguide system, which confirmed the calculations. By a proper setting of the polarisation rotator, the rotation can be corrected and pure X-mode is detected. Temperature profiles have been measured successfully by the polychromator.

Keywords: ECE Diagnostics, Mode Conversion, Large Helical Device

1. Introduction

The electron cyclotron emission (ECE) spectra from magnetised plasmas, in particular tokamaks, have been used for many years to determine the electron temperature profile. The analysis is straightforward. Different spectral components are emitted from a different position in the plasma, depending on the magnetic field. Two polarisation modes exists for ECE waves: X-mode with the electric field vector perpendicular to the magnetic field and O-mode with a parallel electric field vector. The two polarisation modes have different refractive indices and, hence, propagate differently through the plasma towards the diagnostic antenna. A specific harmonic and polarisation mode of the spectrum is monitored, which is optically thick, such that its intensity is proportional to the temperature.

However, the situation is more complex in the Large helical Device (LHD: R_{ax}=*3.75* m, *a=0.6-0.9* m B_{ax}=*1.5-3* T). The magnetic field configuration of a helical system, like LHD, differs from that of a tokamak. The field strength is a non-monotonic function of the radius, hence one frequency can be emitted at various positions in the plasma. Furthermore, the magnetic field is highly sheared. This large shear causes the propagation of the two polarisation modes to be coupled, with as a result mode conversion and polarisation rotation. The polarisation effects of the LHD plasma have been studied numerically [1]. A brief overview of the results will be given in this paper.

Beside a heterodyne radiometer [2,3,4] and Michelson interferometer [2,4], a grating polychromator is used to measure the ECE spectrum. The details of the diagnostic apparatus will be described in section 2. Experiments have been carried out in order to determine the polarisation of the ECE spectrum. In section 3 the results will be discussed and compared with the theoretical calculations. In section 4 it will be shown that electron temperature profiles can be resolved using the ECE spectra from LHD.

2. The grating polychromator at LHD

The advantages of a grating polychromator (GPC) are the high temporal resolution and the possibility to utilise the system over a broad wavelength range: $(\lambda_{max} - \lambda_{max})/\lambda_{centre} = 0.4$. The grating polychromator at LHD is set-up in a Czerny-Turner mount in order to avoid a large stray-light level. Grating polychromators have been applied to diagnose ECE radiation on various devices. A 14-channel system is presently operated at LHD that will be described below.

2.1 The waveguide system

The microwaves are received via the ECE diagnostic antenna and is *60m* circular oversized waveguide system [2]. The antenna views the plasma in the equatorial plane. A polarisation rotator and a polarisation splitter directs the appropriate polarisation mode towards the GPC. It was measured that a linear polarised wave rotates its polarisation over *33°* while being transmitted through the waveguide. As will be discussed later, the LHD plasma itself may also cause a polarisation rotation. The polarisation rotator can be used to correct for these effects. Before the entrance to the polychromator two low-pass-filters prevent higher order mode radiation (The cut-off frequencies are: $f^{co} = 248$ *GHz* and $f^{co} = 168$ *GHz*). In order to prevent damage by high power ECH sources, a notch filter was installed in the waveguide system [2].

2.2 The grating polychromator

Fig 1. shows the set-up of the grating polychromator. The circular waveguide is tapered to rectangular WR284. The electric field vector of the wave is directed horizontally. The microwaves enter via slit of *12 × 34.85 mm* and two small mirrors (*M1/M2*). Via a collimating mirror (*M3: 300 × 300 mm*) the microwave beam is focused on the grating (*G: 300 × 300 mm*). The grating consist of vertical grooves with a blaze angle of: $\theta_{blaze} = 20°$. It has an efficiency of *0.7 - 0.9* in the wavelength range: $\lambda/d = 0.5 - 1.2$, i.e. ($d = 3$ mm) $f = 200 - 83$ GHz. Gratings with a groove constant of $d = 2.3$, *3* and *5 mm* can be applied. The angle of the grating can be adjusted mechanically. The blazed grating scatters its refraction pattern on a large focusing mirror (*M4: 600 × 300 mm*) with a focus point of $R = 1500$ *mm*.

2.2 Detectors and data acquisition

The mirror (*M4*) directs the different wavelengths into 14 detector entrance slits of: *10.2 × 50 mm* (E-band waveguides), which are connected to the detectors. Each channel has a spectral resolution of $\Delta f^{FWHM} = 2.5$ GHz. The 14 liquid He-cooled detectors InSb diodes are mounted in a cryostat.

Low-noise pre-amplifiers, with a tuneable gain of *40* or *60* dB, are directly mounted on the cryostat. The signals are fed to the main amplifier/filter bank with gain settings of *1, 3, 10* × and filter settings of *10, 100* kHz and *1* MHz. The output can be digitised with a sampling rate of *250* kHz for *2* s. For long pulse operation additional data is stored with a sampling rate *10* kHz.

3. The polarisation of electron cyclotron emission spectrum

The plasma is a refractive medium for microwaves. While the ECE waves travel from the resonance, where they are emitted, towards the antenna, they can be refracted, re-absorbed or

reflected. Because X and O-mode have different refractive indices, their propagation differs too.

LHD has a specific magnetic field configuration (see Fig. 2). It has a maximum in the centre and a large shear (B^{pol}/B^{tor} is of order unity at $r=a$). Thus, each frequency, emitted at a different position, will have its X-mode polarisation under a different angel in the laboratory frame. Furthermore, the shear causes the propagation of the two polarisation modes to be coupled [5].

3.1 Coupled propagation in LHD

If $E_{//}$ and $E_{\perp}$ are the local electric fields of O and X-mode wave, the coupled wave equations of both modes can be written as [5]:

$$\frac{d^2E_{//}}{dr^2}+(\frac{\omega^2}{c^2}N_X^2-\phi^2)E_{//}=+2\phi\frac{dE_{\perp}}{dr}+E_{\perp}\frac{d\phi}{dr},$$

$$\frac{d^2E_{\perp}}{dr^2}+(\frac{\omega^2}{c^2}N_O^2-\phi^2)E_{\perp}=-2\phi\frac{dE_{//}}{dr}-E_{//}\frac{d\phi}{dr},$$

where, N_x and N_o, are the refractive indices for X and O-mode, respectively and ϕ is the gradient of the magnetic shear (see Fig. 2). In tokamak plasmas, were the shear is negligible, one finds the wave equations to be uncoupled. The coupled wave equations were solved for typical ECE frequencies, along their path towards the antenna. At the resonance, absorption and emission were determined according to the proper absorption and emission constants [6].

It was found that strong mode conversion occurred in low-density plasmas ($n_e < 0.25\ 10^{19}$ m^{-3}). However, at higher densities the orientation of the waves electric field vector rotated with the sheared magnetic field in the laboratory frame. In the case of X-mode it remained perpendicular to the field and mode conversion was negligible. In Fig. 3 the angle of the polarisation at the plasma edge for all 2nd harmonic frequencies is given for different densities. At low densities all frequencies exit the plasma under different angles, but at higher densities they undergo polarisation rotation, and exit under approximately the same angle, $\alpha=35°$. Polarisation rotation becomes stronger if the refractive indices of X and O-mode differ, and hence depends indirectly on the density.

Polarisation rotation is profitable, because, X and O-mode can de separated in LHD. Calculations showed that due to the large optical thickness of 2nd harmonic X-mode, wall reflections and emission from the second resonance are re-absorbed before they reach the antenna [1,7].

3.3 Experiments on polarisation

Experiments have been performed in order to verify the polarisation the ECE spectrum. During long pulse operation, the polarisation rotator was turned. The setting of the polarisation rotator was monitored by the data acquisition system. The plasma was sustained by Neutral Beam Injection (NBI) for 6 s. A magnetic field of $B_{ax}=2.75$ T was used. The results are plotted Fig. 4. The central density increased from $n_{eo}=1.5$ to $1.8\cdot10^{19}$ m^{-3}, yielding a decrease of the central temperature. The angle of the polarisation rotator is changed between 0 and 120°. One of the Grating Polychromator channels (f = 150 GHz, R_{res} = 3.7 m) is plotted. The optical depth of O-mode is always smaller than, $\tau < 0.03$ but the X-mode emission is optical thick ($\tau > 5$). Thus the intensity for this frequency, usually matches the central electron temperature. However, the rotation of the polarisation causes a large oscillation.

In Fig. 5 the ratio between the radiation temperature and electron temperature is plotted versus the angle. This is the real angle of rotation in the LHD laboratory frame, i.e. the

polarisation rotator angle corrected by the offset rotation (see 2.1) in the total waveguide system. An oscillation is observed with a maximum at, $\alpha = \theta(a) \approx 35°$, when $T^{rad} = T^{x} = T_{e\omega}$. While a minimum is found if pure O-mode is detected. The O-mode intensity is about *70%* of that of X-mode. This high level can be explained by wall X-mode waves that are converted to O-mode upon reflection at the wall, which can propagate without re-absorption through the plasma [1,7]. At intermediate angles a mixture of X and O-mode is measured. The radiation temperature as a function of the polarisation rotator angle, α, for a given spectral component ω, can be given by,

$$T(\alpha) = T^{x} \cos^2(\alpha - \theta(a)) + T^{o} \sin^2(\alpha - \theta(a)),$$

where it is assumed that the wave undergoes perfect polarisation rotation up to the edge of the plasma. If the X-mode is optically thick and the intensity and the O-mode is *70%* of that of X-mode (calculated with an arbitrary reflection coefficient of the LHD wall of $\rho=0.95$ and a mode conversion fraction of $\pi=0.1$ caused by the reflection [1,7]), the above equation can be plotted in Fig. 5. A nice match between the measured and calculated curve is found.

4. Temperature profiles

During standard operation the polarisation rotator is set, such that it corrects for the rotation caused by the plasma, and hence, X-mode is fed to the GPC. Small variations in the polarisation angle, caused by changes in the magnetic field configuration, the position of the plasma edge, or non-perfect polarisation rotation are found to be negligible during normal operation.

Temperature profiles have been measured successfully by the grating polychromator during the last experimental campaigns of LHD. The first measurements will be discussed in this section. Discharges with $B_{ax}=2.75$ T have been analysed using a grating constant of $d = 3$ mm (incident angle of *-4.4* °) covering the frequency range of, *150 - 100* GHz. A radial coverage of, $r/a = 0 - 0.89$ was achieved. Because the magnetic field is a non-monotonous function of the radius in LHD (see Fig. 2) only information of the outside ECE resonance, and thus, half of the temperature profile can be obtained by the GPC. A second antenna, viewing from the opposite side, is required to reveal the inside profile [4].

4.1 Cross-calibration and comparison with Thomson scattering

The GPC is cross-calibrated against temperature profiles measured by the Thomson scattering diagnostic. For this purpose high density discharges ($n_e > 2 \cdot 10^{19}$ m^{-3}) are used, heated by neutral beam injection (NBI) with central electron temperatures of 2 keV.

The temperature profiles measured by Thomson scattering and the GPC matched over a large parameter range: $n_e > 1.0 \cdot 10^{19}$ m^{-3} and $T_e = 1 - 3.5$ keV. A comparison is shown in Fig. 6, where the temperatures of 3 GPC channels (ch. 13: $r/a = 0.08$, ch 8: $r/a=0.49$, ch4: $r/a=0.74$) compared with that given by Thomson scattering. The temperatures of the 2 discharges which are plotted decreased in time.

4.2 Measurements during ECH

The use of electron cyclotron heating (ECH) highly disturbed the grating polychromator signals. The plasma is initially ionised by ECH ($f=83$ GHz). In this initial low-density phase, extreme radiation temperatures up to *8* keV were detected, due to ECH generated non-thermal electrons.

During simultaneous heating of high density plasmas ($n_e > 1.5 \cdot 10^{19}$ m^{-3}) by NBI and ECH non-thermal electrons did not affect the measurement. Nevertheless, it was found that ECH also disturbed the GPC signals directly by an increased stray-light level. It caused a sudden jump in signal when ECH was switched on or off. Fluctuations in the stray-light level enhanced the noise. Although the monitored frequencies are far from the ECH frequency still several *10* eVs of stray-light were detected, despites of the notch filter in the waveguide. The averaged stray light level increased for lower frequencies, closer to the ECH frequency. At higher densities, when more ECH power is absorbed in the plasma, the stray-light decreased.

4.3. Temperature profiles during NBI

Temperature profiles have been measured during neutral beam injection. During NBI heating the density is generally higher than ($n_e > 1.0 \cdot 10^{19}$ m^{-3}) thus the outer resonance is sufficient optically thick.

Typical density profiles in LHD are flat, or slightly hollow, yielding quite peaked temperature profiles. Over a wide range of densities and temperatures, the temperature profile shape is very rigid. A characteristic LHD temperature profile with the almost triangular shape: $T(r/a) = T_0(1-(r/a)^{1.36})$ was found by fitting to the profile data.

Changes in the profile shape have been observed during central heating by ICH and after pellet injection. In the last case, cooling of the plasma edge by radiation and extreme hollow density profiles yielded a peaking of the temperature profile.

In Fig. 7 an example is shown of the temporal behaviour of the temperature profile. In this discharge (#8733) *5* pellets were injected, yielding an increase in density and a subsequent decrease in temperature. The plasma energy reached *754* kJ at the end of the NBI phase. After each pellet, a hollow density profile caused a fast peaking of the temperature profile. The change in profiles can be clearly seen in Fig. 8a and b. The profiles are shown at $t=0.81$ s, just after the before the pellet and at $t=0.82$ s. The hollow density profile results in a peaking of the temperature profile.

5. Conclusions

The large shear of the magnetic field in LHD might cause problems for the analysis of ECE spectra. The effect of the polarisation due to this large shear has been studied numerically as well as experimentally, by means of a polarisation rotator and a 14-channel grating polychromator.

At high enough density, mode conversion was found to be negligible. Calculations showed that in this case the polarisation of the ECE waves rotate in the laboratory frame. This rotation has been confirmed experimentally. If this rotation is not taken into account, a mixture of X and O-mode will be detected. A polarisation rotator is set in the waveguide system to correct for this effect.

Hence, 2nd harmonic X-mode spectra can be monitored. Temperature profiles have been successfully measured by the LHD grating polychromator.

Acknowledgements

The work presented in this paper has been performed with financial support of the Japan Society of Promotion of Science and the National Institute for Fusion Science.

References

[1] P.C. de Vries, et al, in the Proc. of the 26th Conf. on Plasma Phys. and Contr. Fusion, Maastricht (1999) Part II, p 25.
[2] Y. Nagayama, et al., Rev. Sci. Instrum. 70 (1999) 1034.
[3] S. Inagaki, et al., in the Proc. of the 26th Conf. on Plasma Phys. and Contr. Fusion, Maastricht (1999) Part III, p 105.
[4] Y Nagayama, et al., Overview of ECE diagnostics on LHD, in this proceedings.
[5] I. Fidone and G. Granata, Nucl. Fusion 11 (1971) 133.
[6] M. Bornatici, et al., Nucl. Fusion 23 (1983) 1153.
[7] P.C. de Vries, et al, submitted to Phys. Plasmas (1999).

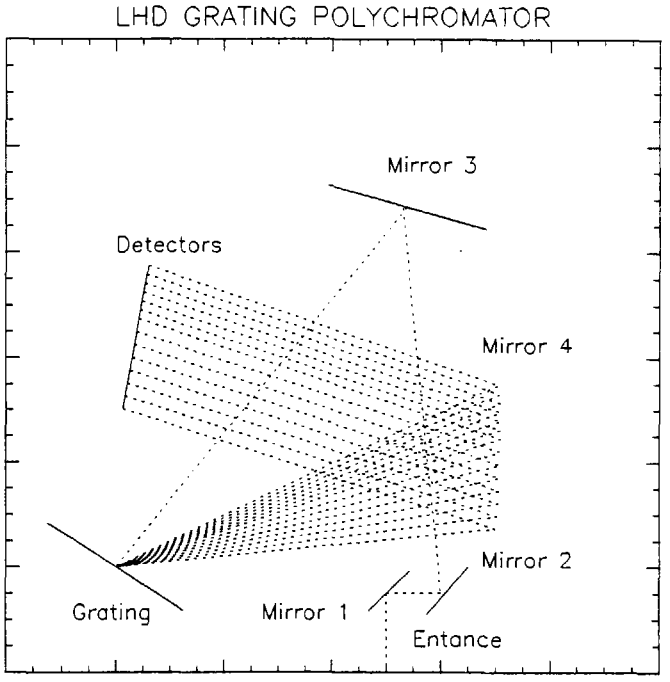

Fig. 1: Schematic drawing of the LHD grating polychromator

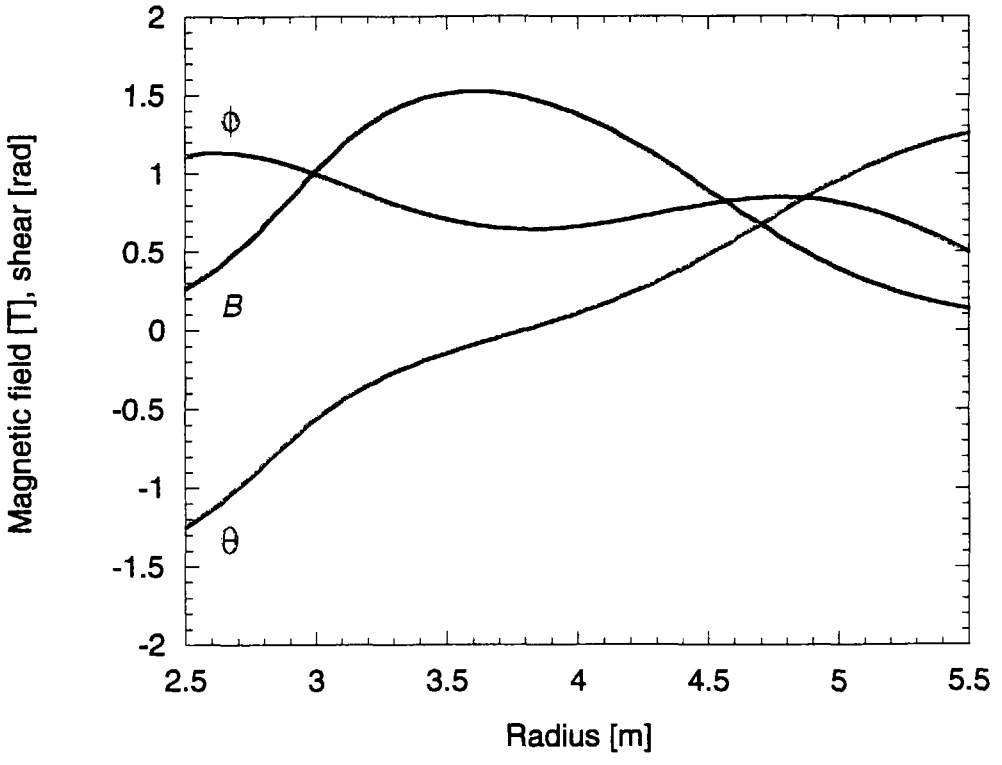

Fig. 2: The magnetic field configuration in the line-of-sight of the diagnostic antenna. The magnetic field amplitude, the shear, $\theta \equiv atan(B^{pol}/B^{tor})$, and its derivative, ϕ, are plotted.

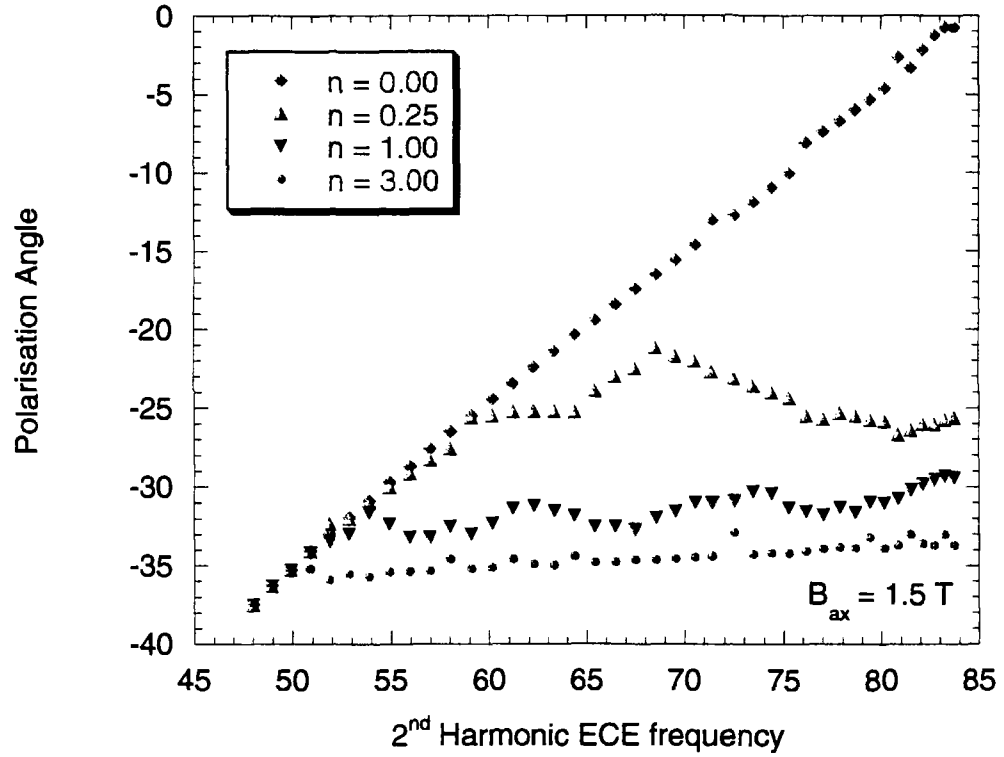

Fig. 3: The polarisation angle (angle of an X-mode waves electric field vector) at $r=a$ calculated for each spectral component using different plasma densities.

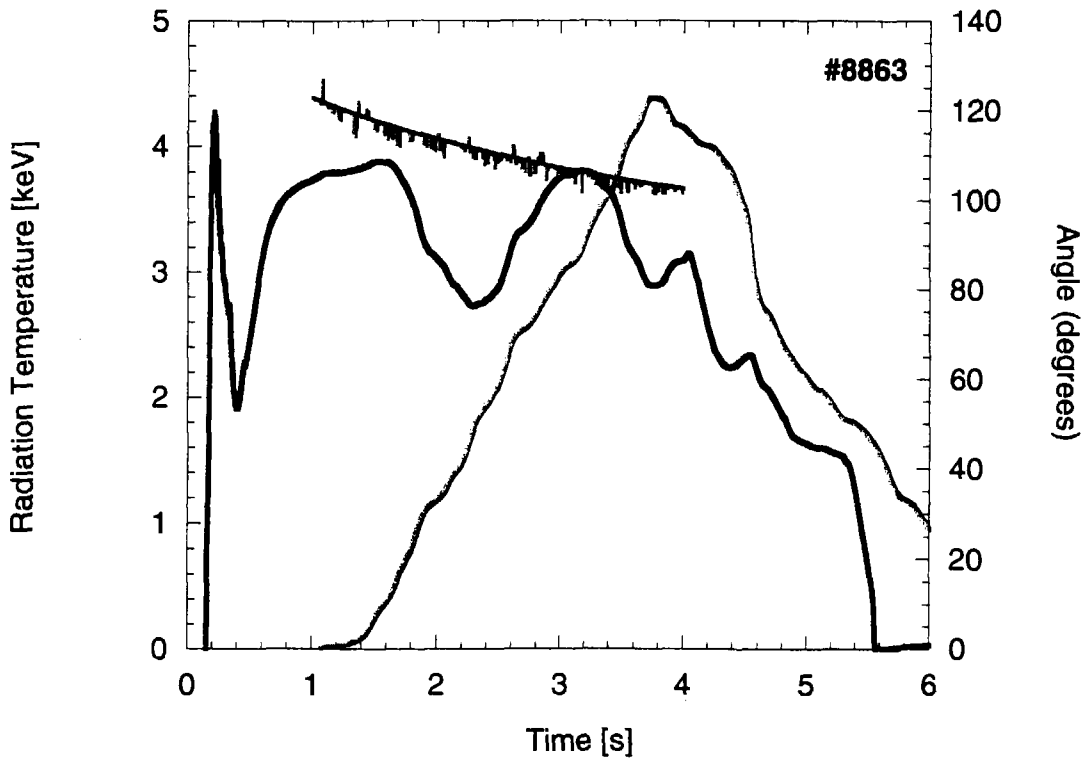

Fig. 4: The radiation temperature of the central CPC channel (#13) (blue curve), the central temperature and the polarisation rotator angle (red curve) are shown for discharge #8863.

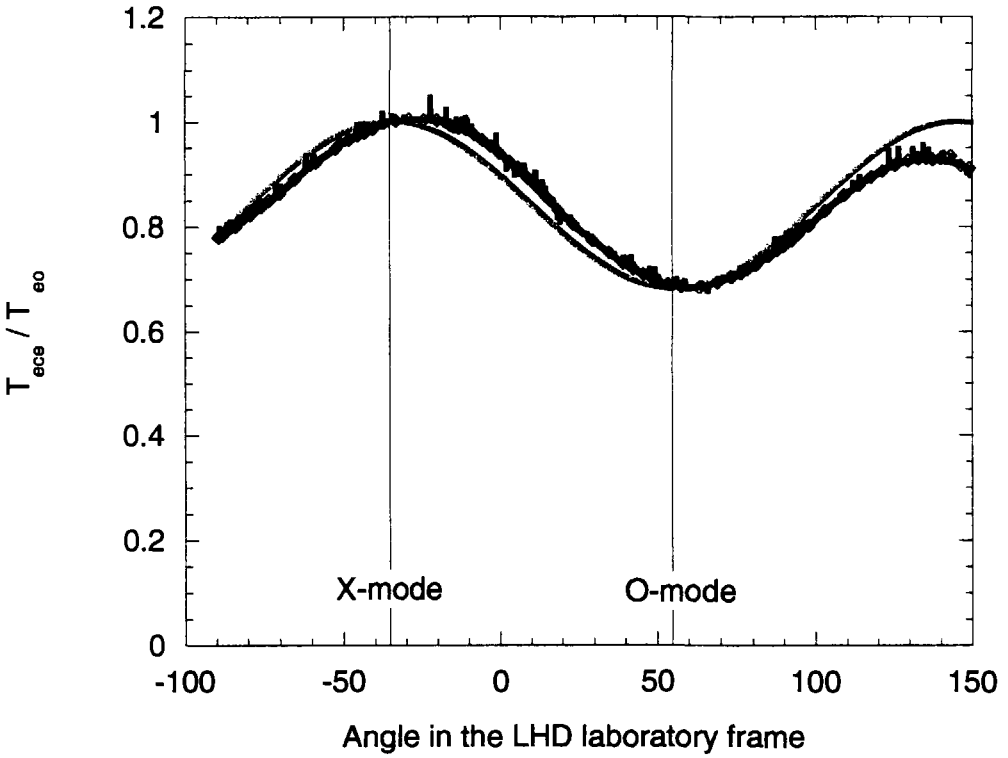

Fig. 5: The ratio between the ECE radiation temperature and the electron temperature, as a function of the polarisation angle in the LHD laboratory frame, together with the calculated curve are plotted.

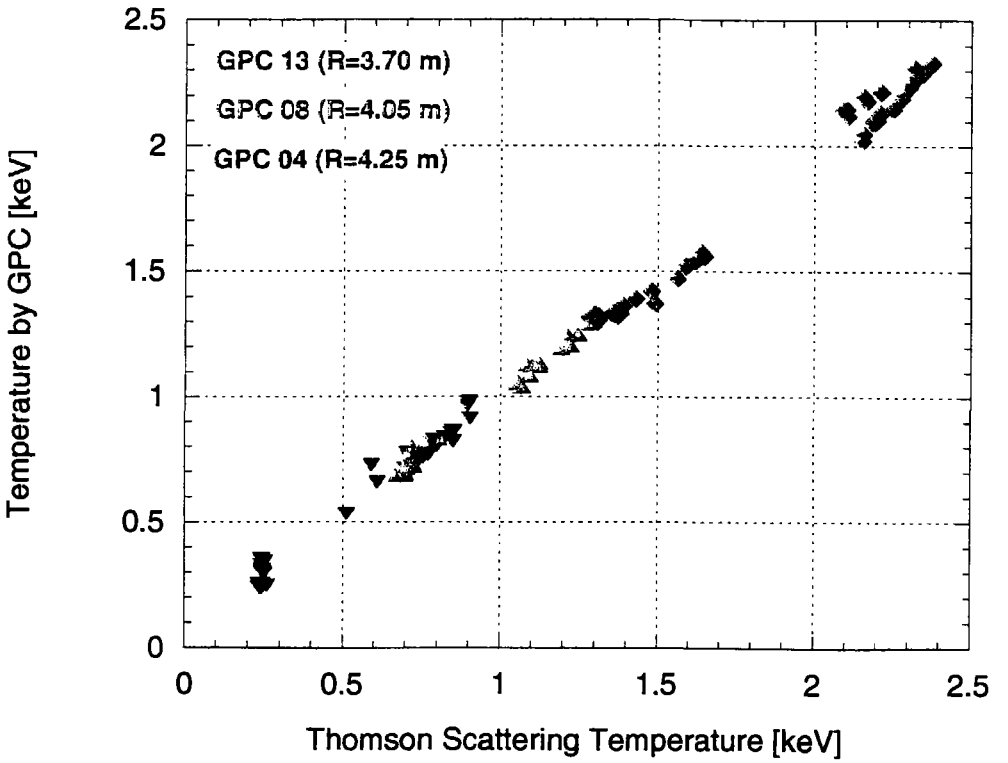

Fig. 6: Comparison of Thomson scattering and temperatures measured by the GPC for three different channels.

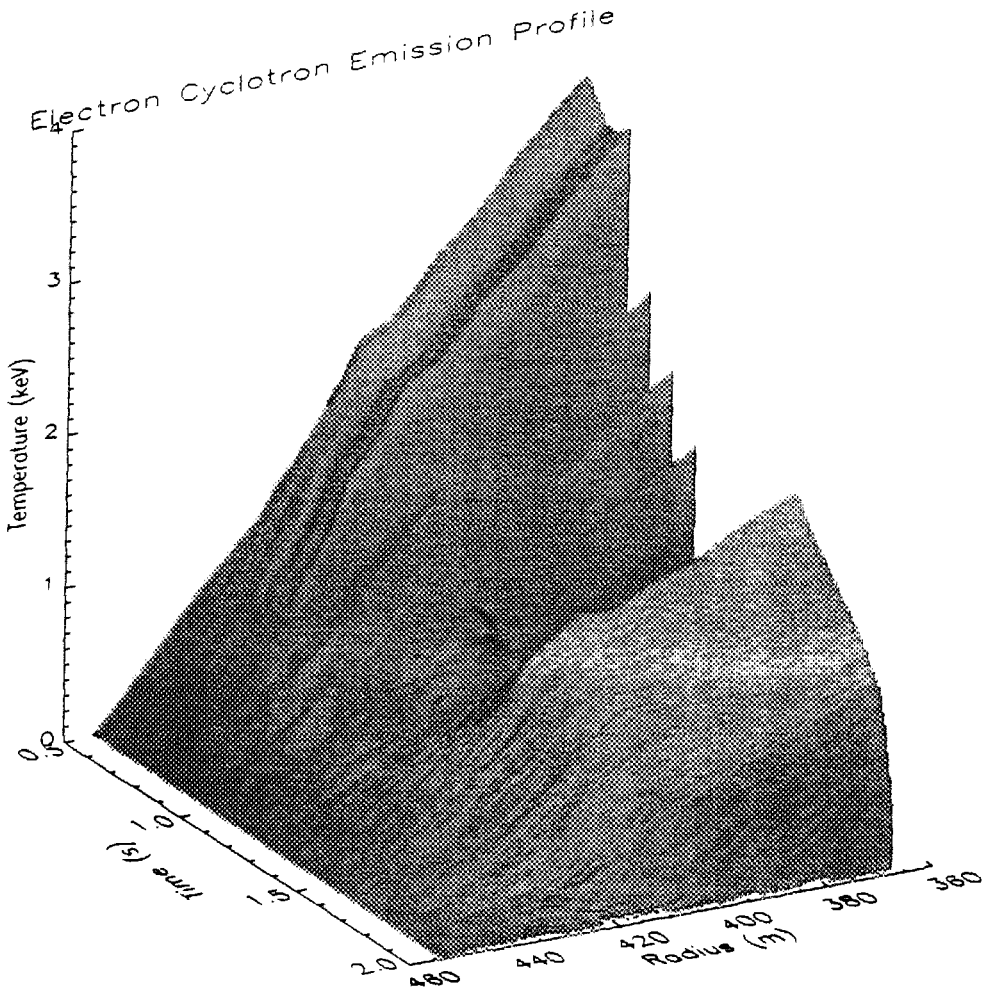

Fig. 7: The temporal behaviour of the electron temperature of discharge #8377. The initial ECH phase is omitted in this plot. Injection of pellets results in a collapse of the temperature.

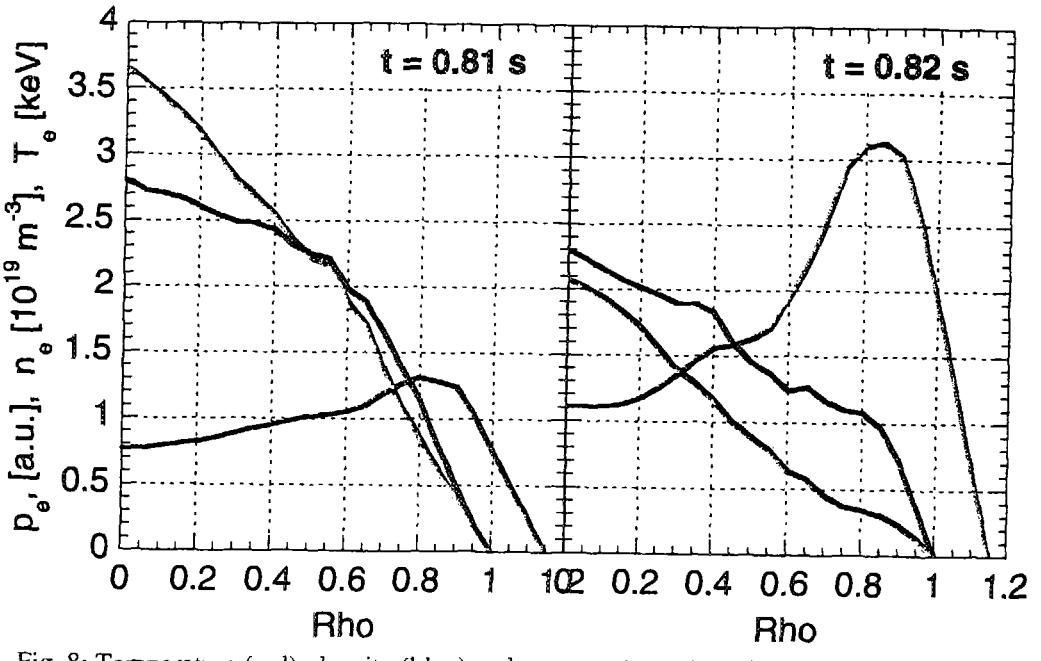

Fig. 8: Temperature (red), density (blue) and pressure (green) profiles of discharge #8733, at *t=0.81* s and *0.82* s